

# Dynamics of chiral fermions and chiral magnetic effect\*

Qiang Li

Department of Physics and Astronomy, Stony Brook University  
Condensed Matter Physics and Materials Science Division, Brookhaven National Laboratory

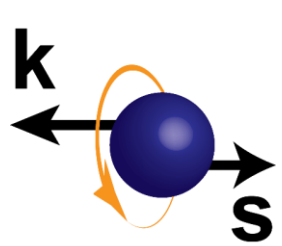
\*The work at Brookhaven Lab is supported by the U.S. Department of Energy, Office of Basic Energy Sciences, Division of Materials Sciences and Engineering, under Contract No. DE-SC0012704.

# Outline

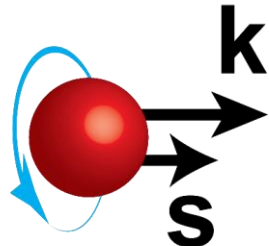
- A brief review of chiral magnetic effect
- Control of topological states in condensed matters
- Massive Dirac semimetals for axions and dark matters detection
- Quantum computing with chiral fermions

# Chirality:

(Relativistic electrons, quarks, and neutrinos)

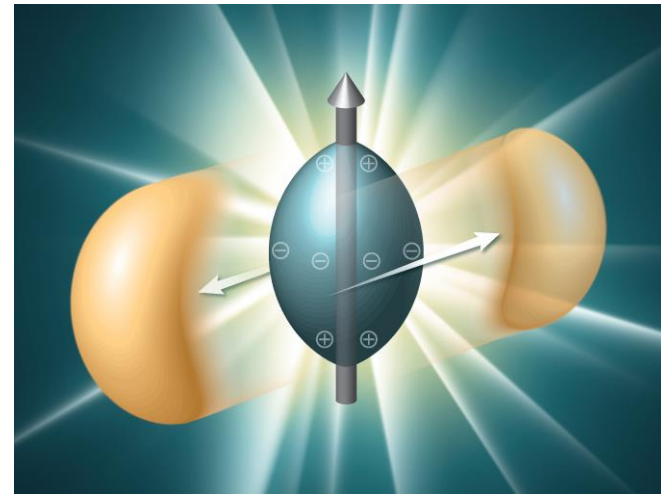


Left-handed



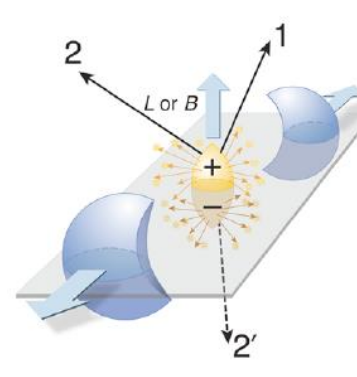
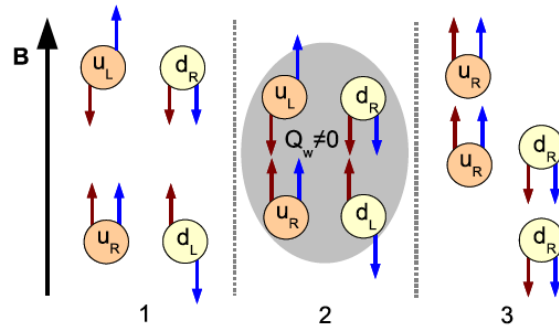
Right-handed

Quark-gluon plasma in heavy-ion collisions  
(RHIC and LHC)

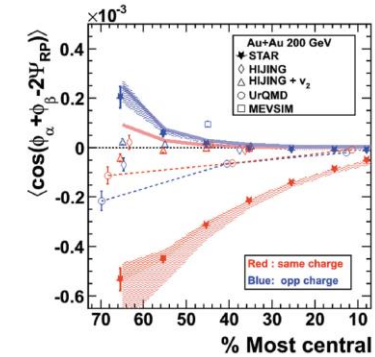


# Chiral magnetic effect (CME)

– the generation of electric current by the chirality imbalance between left- and right-handed fermions in a magnetic field.



(STAR Collaboration)



D. Kharzeev, L. McLerran, H. Warringa, 2007

K. Fukushima, D. Kharzeev, and H. Warringa. Phys. Rev. D, 78, 074033 (2008).

3D semimetals with quasi-particles that have a linear dispersion relation have opened a fascinating possibility to study the quantum dynamics of relativistic field theory in condensed matter experiments.

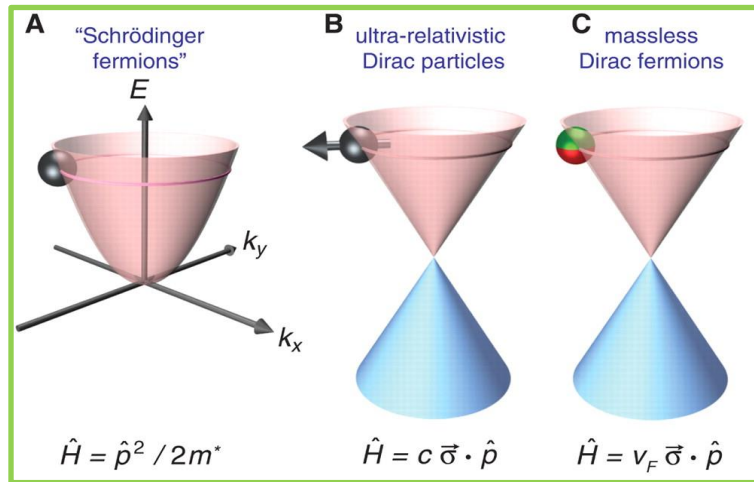
# Chirality:

(electrons, quarks, and neutrinos)



Left-handed

Right-handed



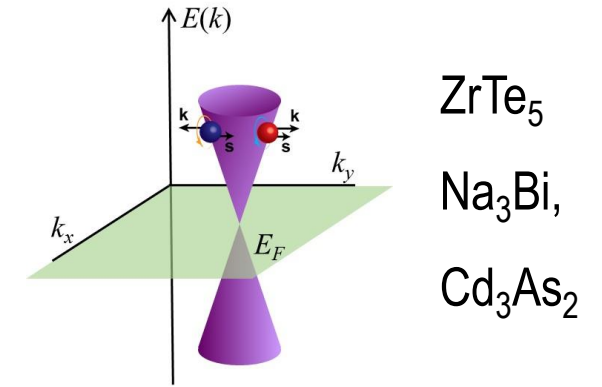
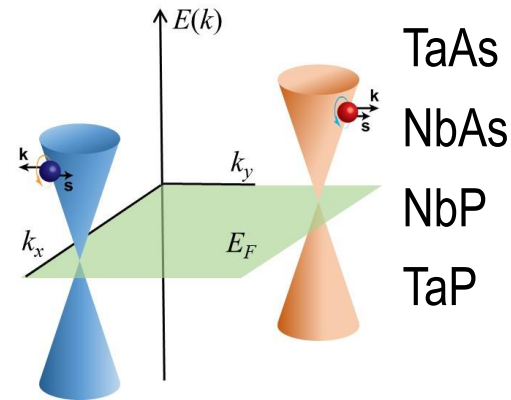
A. K. Geim, Science 324,1530 (2009)

# 3D semimetals with linear dispersion

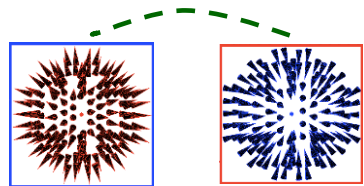
**Weyl semimetal**  
(non-degenerated bands)



**Dirac semimetal**  
(doubly degenerated bands)

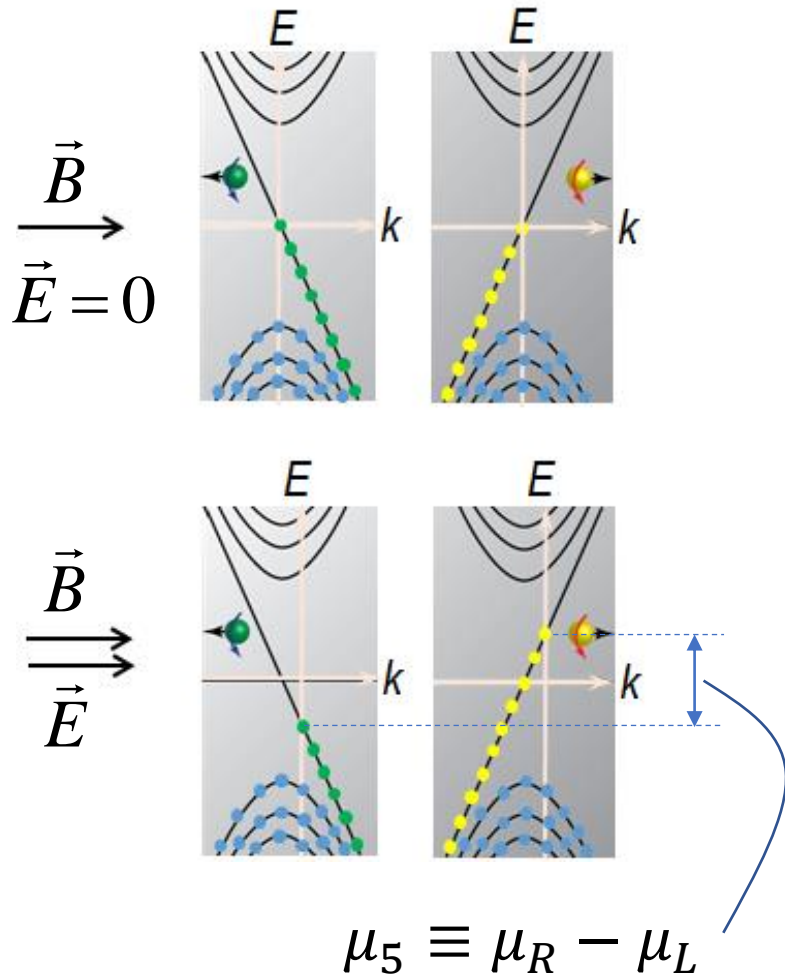


- The Dirac point can split into two Weyl points either by breaking the crystal inversion symmetry or time-reversal symmetry.
- Each Weyl point acts like a singularity of the Berry curvature in the Brillion Zone – magnetic monopole in  $k$ -space



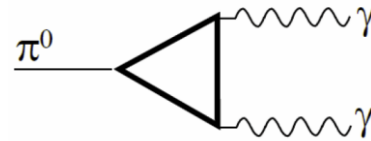
# Chiral anomaly and chiral magnetic effect

$$\vec{J}_{CME} = \frac{e^2}{2\pi^2} \mu_5 \vec{B}$$



## Adler-Bell-Jackiw anomaly

Adler, Phys. Rev. 177, 2426 (1969)  
Bell & Jackiw, Nuov Cim 60, 47-61 (1969)



Rapid decay of  $\pi^0$  into two photons  $\gamma$

## Nielsen and Ninomiya (1983)

- Physics Letters B130, 389 (1983)

“The Adler-Bell-Jackiw anomaly and **Weyl** fermions in a crystal”

## Son and Spivak (2013)

- Phys. Rev. B, 88, 104412 (2013).

“Chiral anomaly and classical negative magnetoresistance of Weyl metals.”

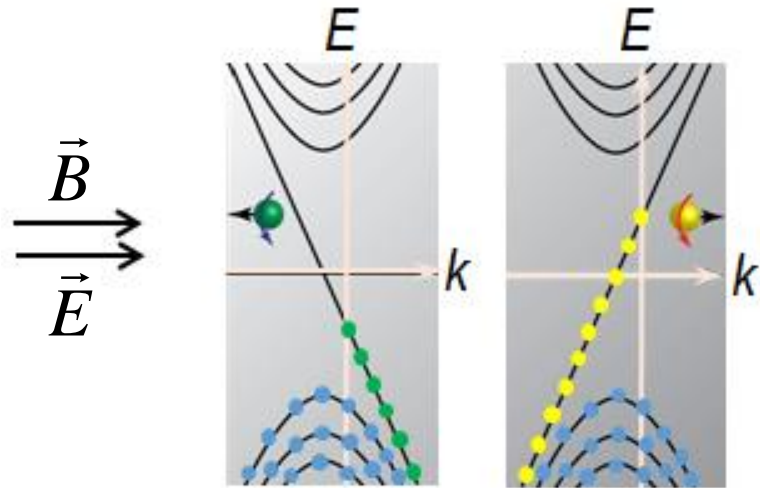
## Burkov (2014)

-Phys. Rev. Lett., 113, 247203 (2014).

“Chiral anomaly and diffusive magneto-transport in Weyl metals”.

# Chiral Magnetic Effect (CME) in Condensed Matters (CM)

Rate of chiral charge generation:



$$\frac{d\rho_5}{dt} = \frac{e^2}{4\pi^2\hbar^2c} \vec{E} \cdot \vec{B} - \frac{\rho_5}{\tau_v}$$

Chiral anomaly

Chirality-changing scattering time  
(chirality flipping time)

$$\rho_5 = \frac{e^2}{4\pi^2\hbar^2c} \vec{E} \cdot \vec{B} \tau_v \quad \text{at } t \gg \tau_v \text{ (steady state)}$$

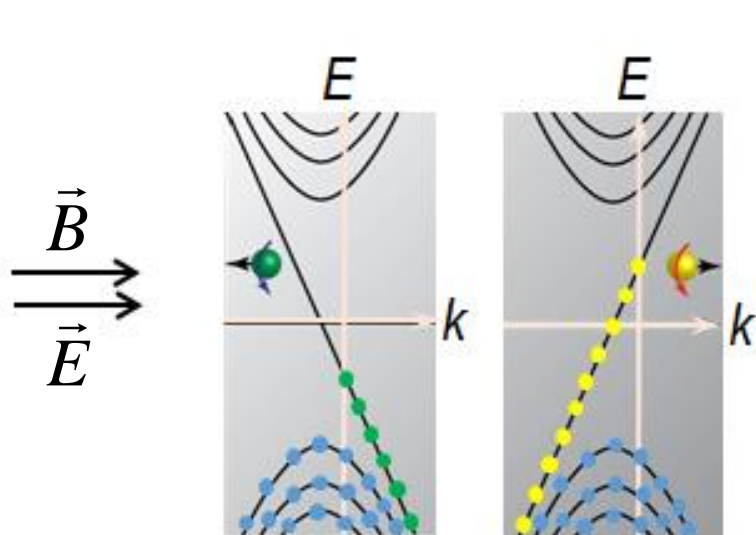
$$\mu_5 = \frac{3}{4} \frac{v^3}{\pi^2} \frac{e^2}{\hbar^2c} \frac{\vec{E} \cdot \vec{B}}{T^2 + \frac{\mu^2}{\pi^2}} \tau_v$$

# Chiral Magnetic Effect (CME) in Condensed Matters (CM)



Dmitri Kharzeev  
(SBU/BNL)

The generation of electric current by the chirality imbalance between left- and right-handed fermions in an external magnetic field.



Chiral magnetic current:  $\vec{J}_{CME} = \frac{e^2}{2\pi^2} \mu_5 \vec{B}$

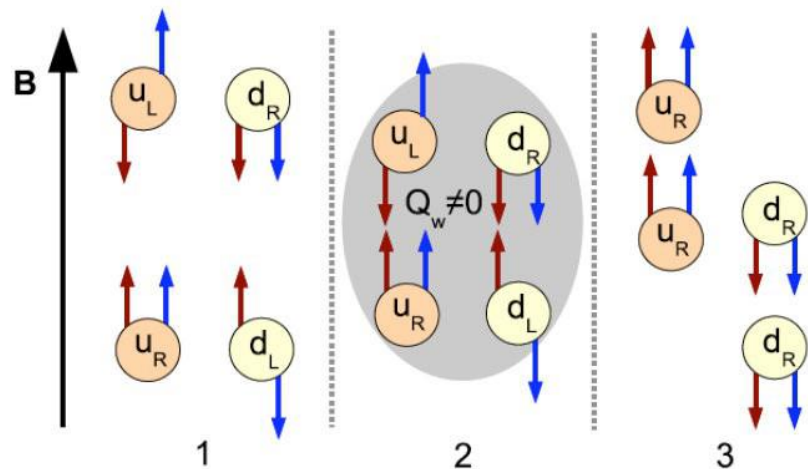
$$J_{CME}^i = \frac{e^2}{\pi\hbar} \frac{3}{8} \frac{e^2}{\hbar c} \frac{v^3}{\pi^3} \frac{\tau_v}{T^2 + \frac{\mu^2}{\pi^2}} B^i B^k E^k = \sigma_{CME}^{ik} E^k$$

$$\sigma_{CME}^{xx} = \frac{e^2}{\pi\hbar} \frac{3}{8} \frac{e^2}{\hbar c} \frac{v^3}{\pi^3} \frac{\tau_v}{T^2 + \frac{\mu^2}{\pi^2}} B^2 = \alpha(T) \cdot B^2$$

**A negative longitudinal magnetoresistance (NLMR) at  $(\vec{B} // \vec{E})$  in Dirac/Weyl semimetals**

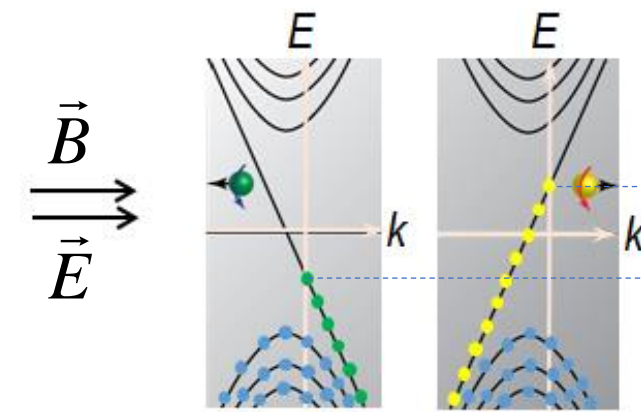
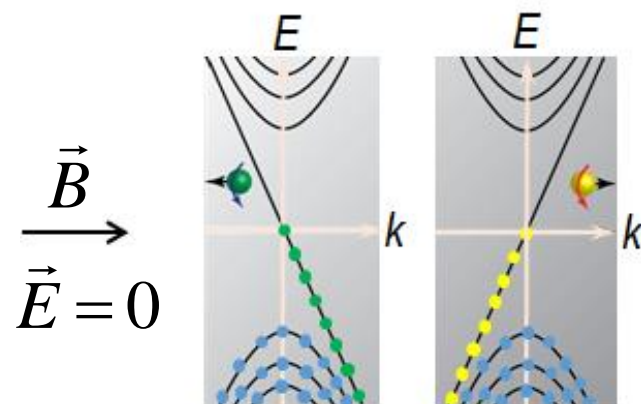
# Chiral magnetic effect

## Quark-gluon plasma in heavy-ion collisions



- Chirality imbalance due to rapid topological transitions mediated by QCD sphalerons (the axial anomaly)
- Huge magnetic field ( $> 10^{12}$  Tesla) due to noncentral collisions
- The induced electric current is proportional to the chiral chemical potential  $\mu_5$  which controls imbalance between left-handed and right-handed quarks

## Chiral fermions in 3D Dirac semimetals



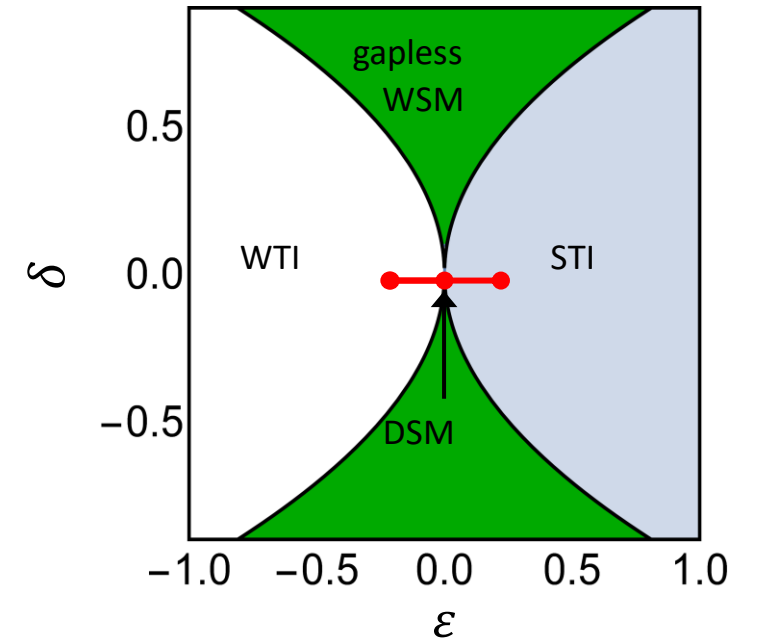
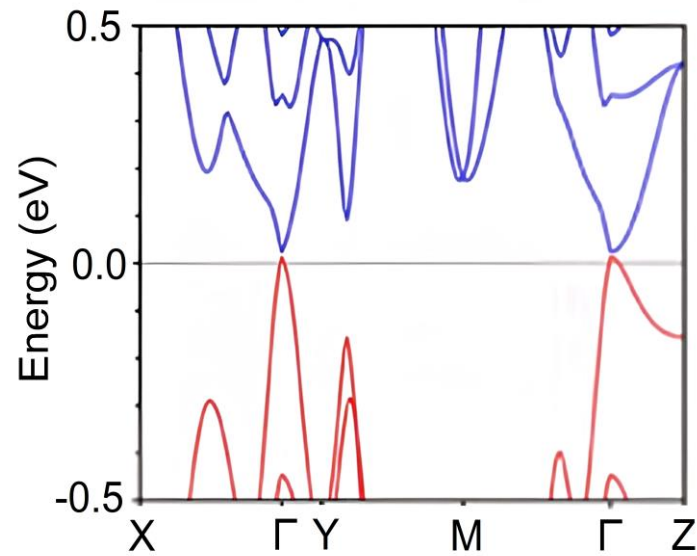
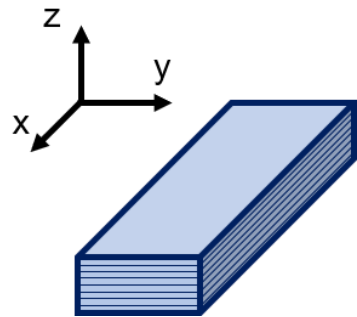
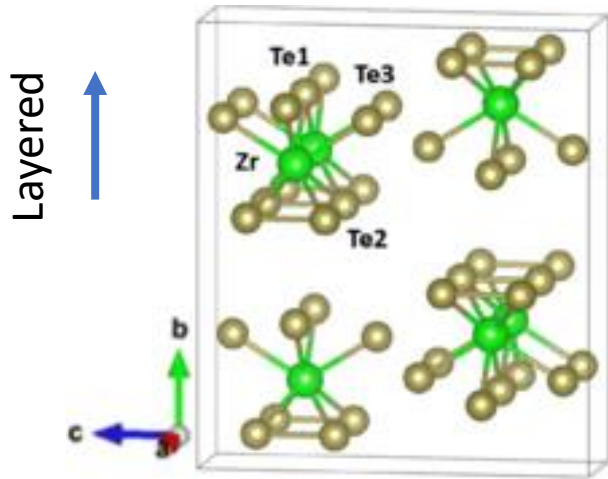
$$\vec{J}_{CME} = \frac{e^2}{2\pi^2} \mu_5 \vec{B}$$

$$\mu_5 \equiv \mu_R - \mu_L$$

**CME is dynamic, not a ground state property**

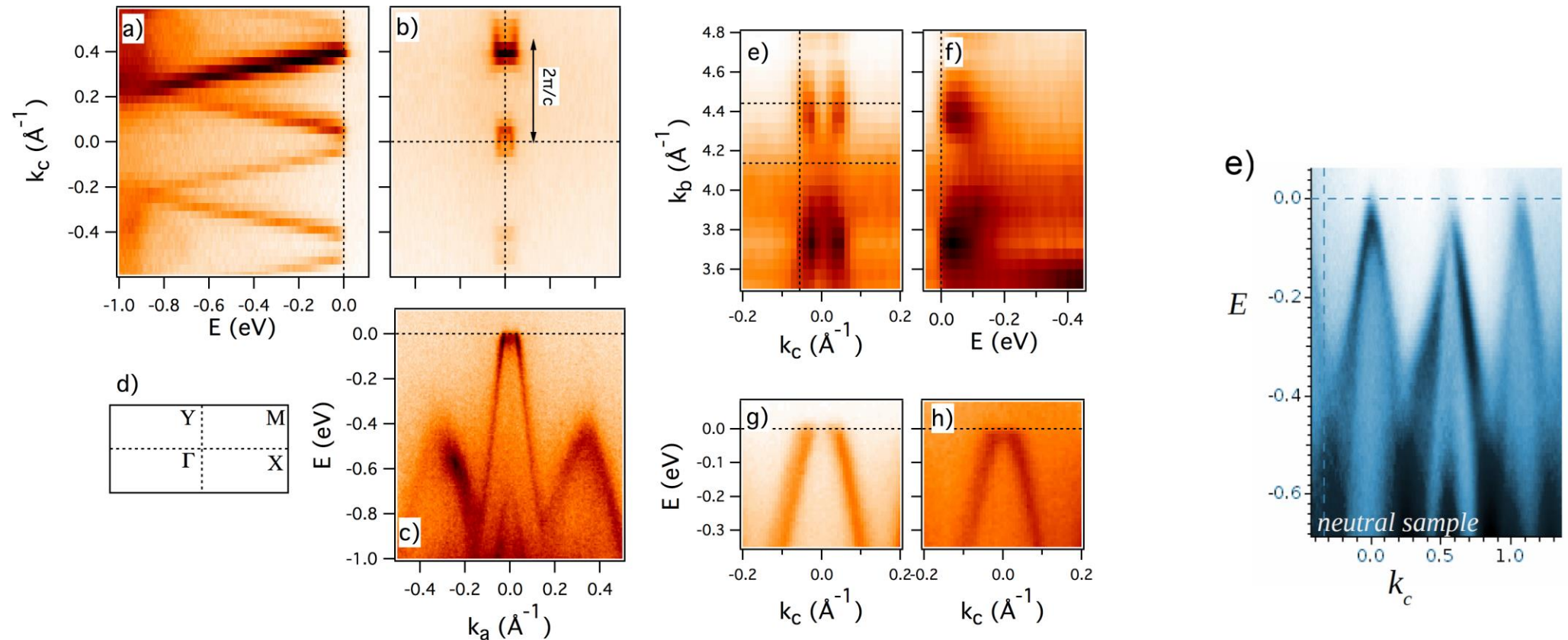


# Discovery of chiral magnetic effect in $\text{ZrTe}_5$



Ref. P. Zhang QL et al., Nat. Commun. 12, 406 (2021)  
N. Aryal, QL et al., Phys. Rev. Lett. 126, 016401 (2021)

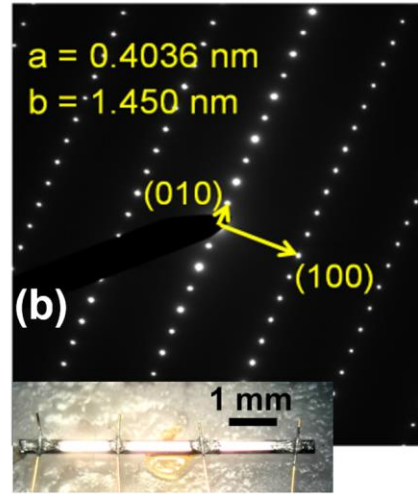
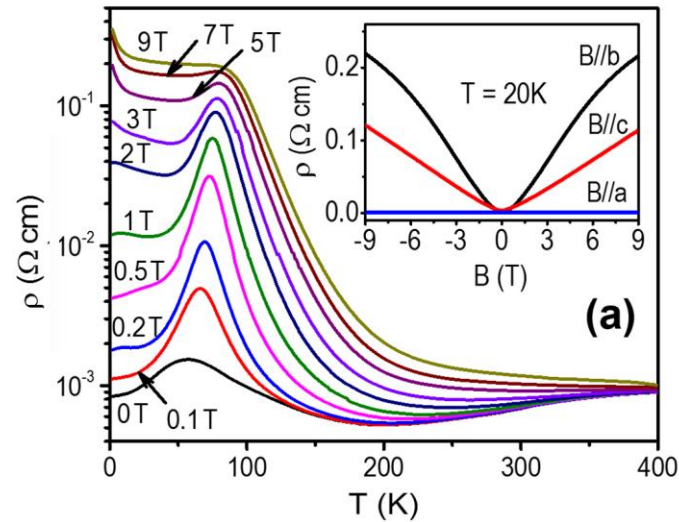
# ARPES results - band dispersion of $\text{ZrTe}_5$



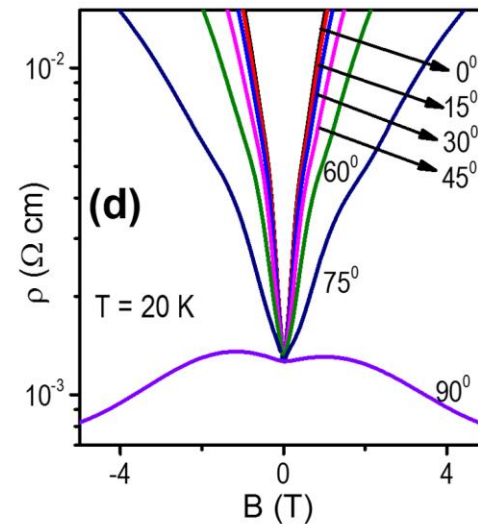
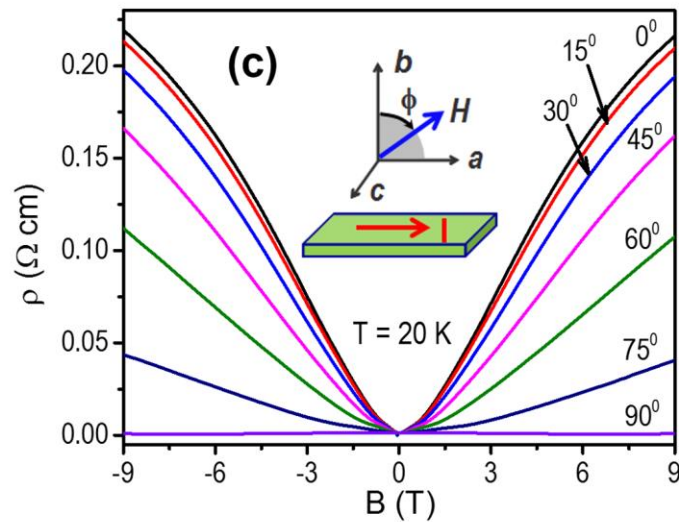
Tonica Valla  
(BNL)

More line 3D Dirac semimetal

# Magneto-transport properties of $\text{ZrTe}_5$

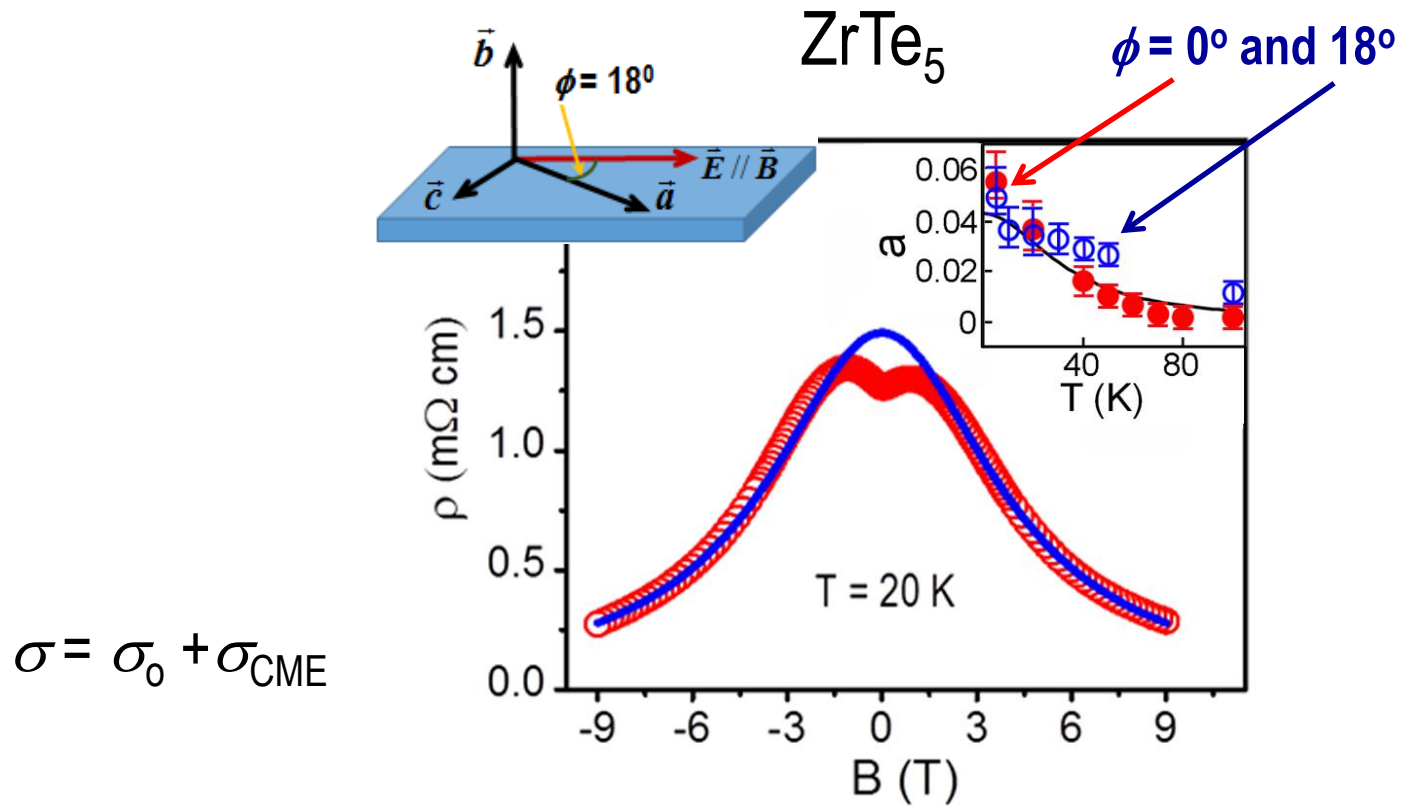


Measurable parameter from CME



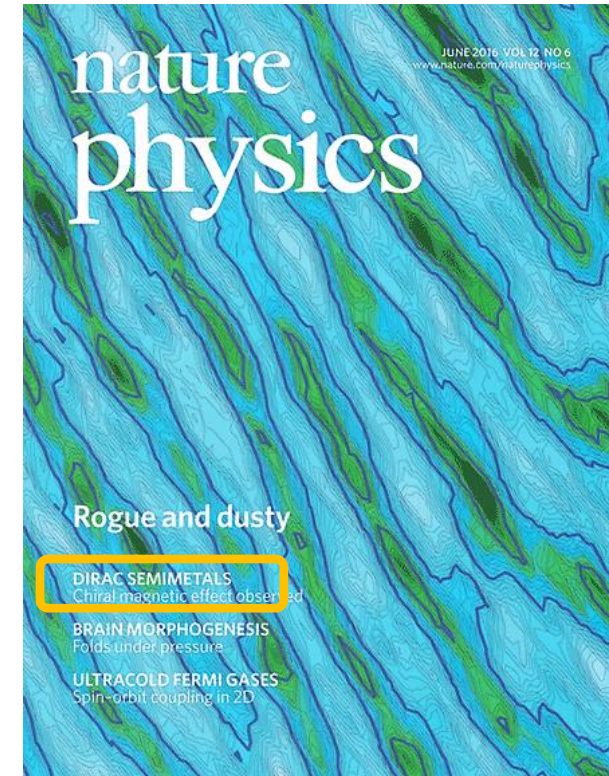
Large negative magnetoresistance  
when  $B//E$  ( $\phi = 90^\circ$ )

# Chiral Magnetic Effect (Chiral Anomaly)



$$\sigma = \sigma_0 + \sigma_{\text{CME}}$$

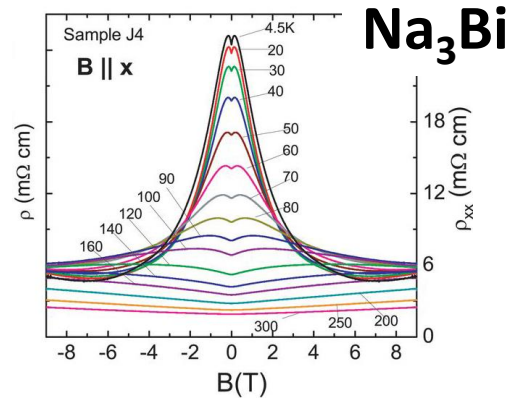
$$\sigma_{\text{CME}}^{zz} = \frac{e^2}{\pi\hbar} \frac{3}{8} \frac{e^2}{\hbar c} \frac{v^3}{\pi^3} \frac{\tau_V}{T^2 + \frac{\mu^2}{\pi^2}} B^2 = a(T) B^2$$



QL, et al arXiv:1412.6543, Nature Physics 12 550 (2016)

# Chiral magnetic effect (chiral anomaly) in Dirac/Weyl semimetals

## Dirac semimetals:

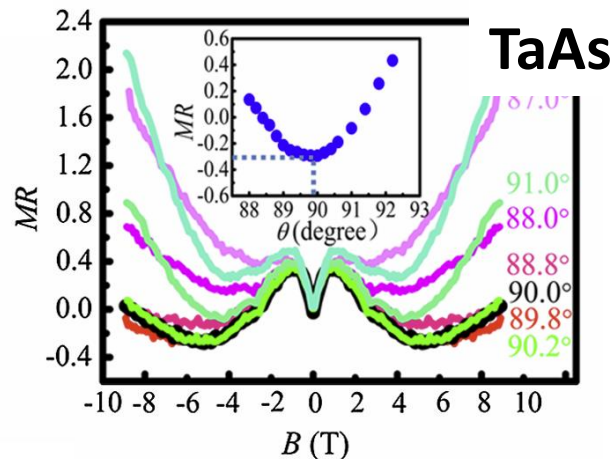


ZrTe<sub>5</sub> - QL, D. Kharzeev et al (BNL and Stony Brook Univ.)  
arXiv:1412.6543; Nat. Phys. 12 550 (2016)

Na<sub>3</sub>Bi - J. Xiong, N. P. Ong et al (Princeton Univ.)  
arxiv:1503.08179; Science 350 413 (2015)

Cd<sub>3</sub>As<sub>2</sub> - C. Li et al (Peking Univ. China)  
arxiv:1504.07398; Nat. Commun. 6, 10137 (2015).

## Weyl semimetals

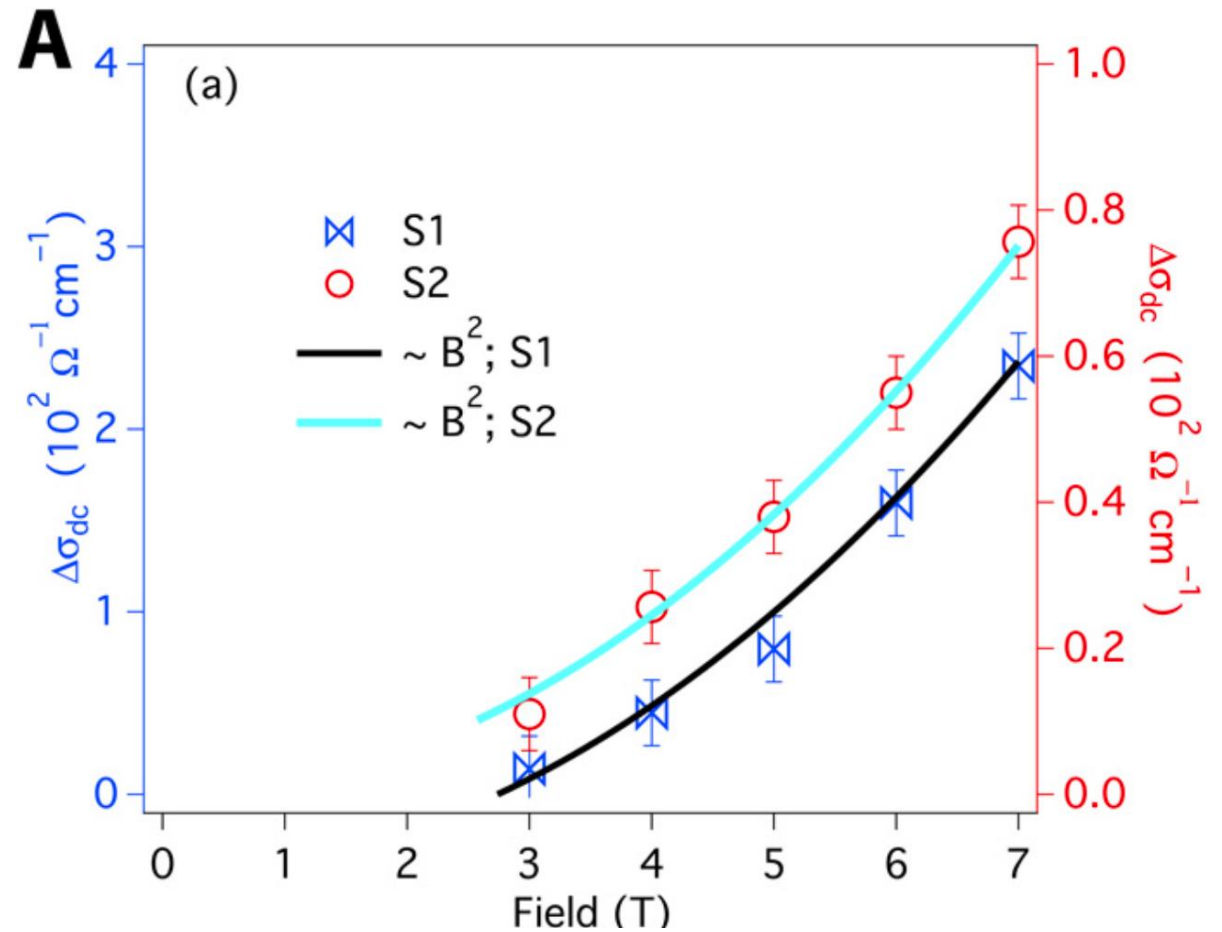


TaAs - X. Huang et al (IOP, China)  
arxiv:1503.01304; Phys. Rev. X 5, 031023

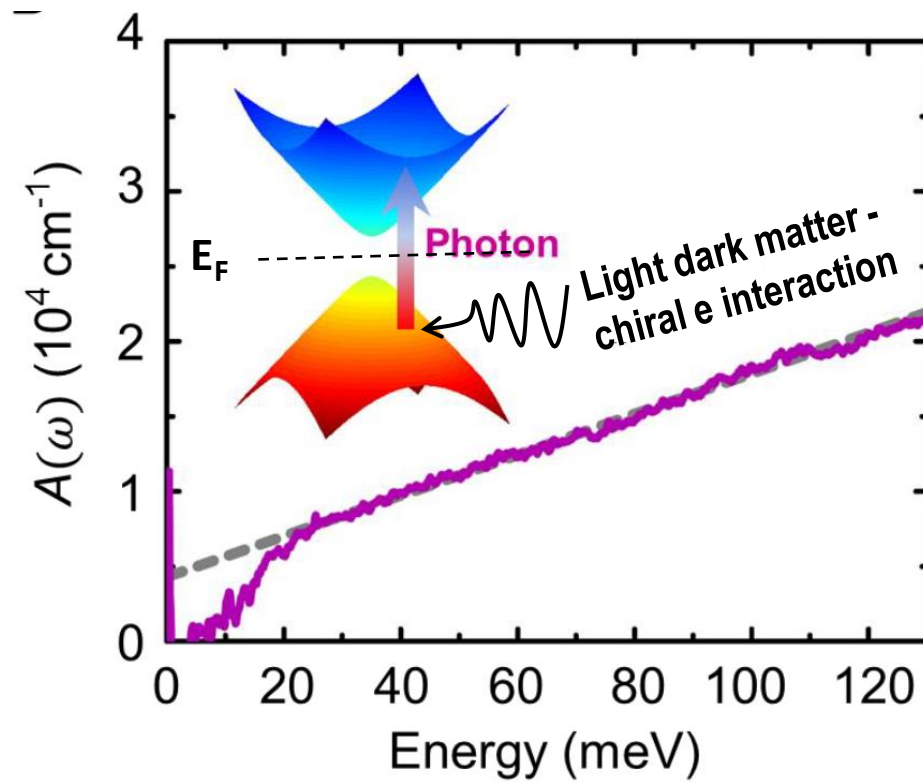
TaP - Shekhar, C. Felser et al (MPI-Dresden)  
arxiv:1506.06577, Nat. Commun. 7, 11615 (2016).

# Magneto-terahertz spectroscopy (non contact) confirmed the chiral anomaly in a Dirac semimetal $\text{Cd}_3\text{As}_2$

“Intrinsic dc magnetoconductivity from chiral anomaly in sample S1 (blue) and sample S2 (red). In both samples,  $\Delta\sigma$  follows  $B^2$ ”



# ZrTe<sub>5</sub> - Light dark matter detection



- At no thermal excitation
- Fermi level in the gap  $\Delta$   
(12.4 meV  $\sim$  3 THz)

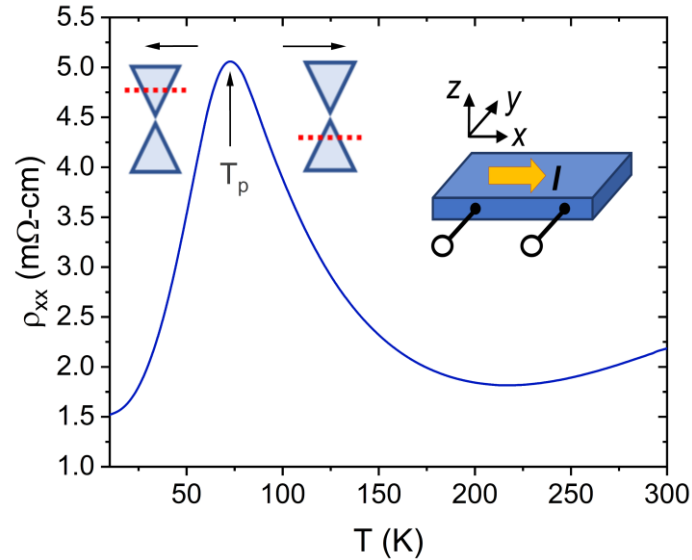
ZrTe<sub>5</sub>



Light dark matter detection

# Temperature induced Lifshitz transition in ZrTe<sub>5</sub>

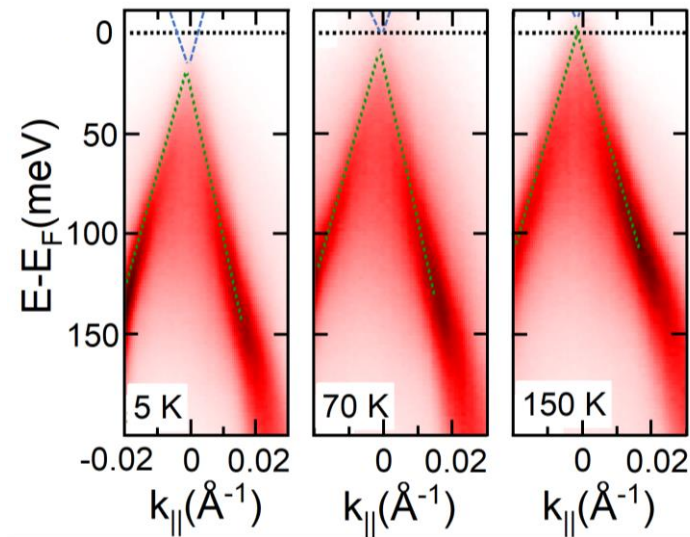
Anomalous resistivity peak in ZrTe<sub>5</sub>



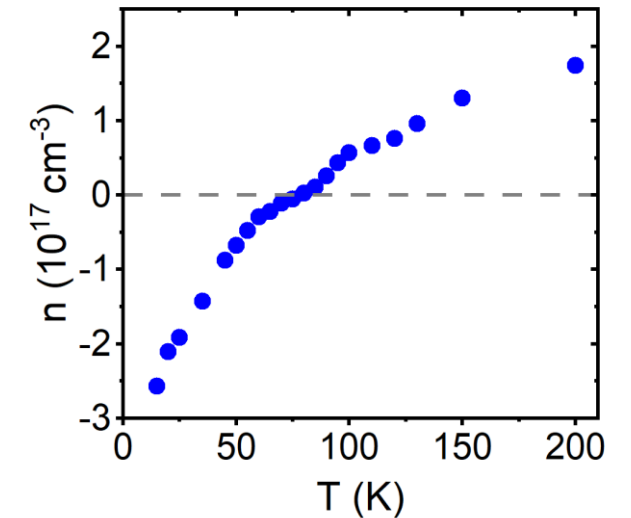
H Chi, QL et al, New Journal of Physics 19, 015005 (2017)

The Fermi level shifts with temperature from the bottom of the conduction band to the top of the valence band.

From ARPES measurements:



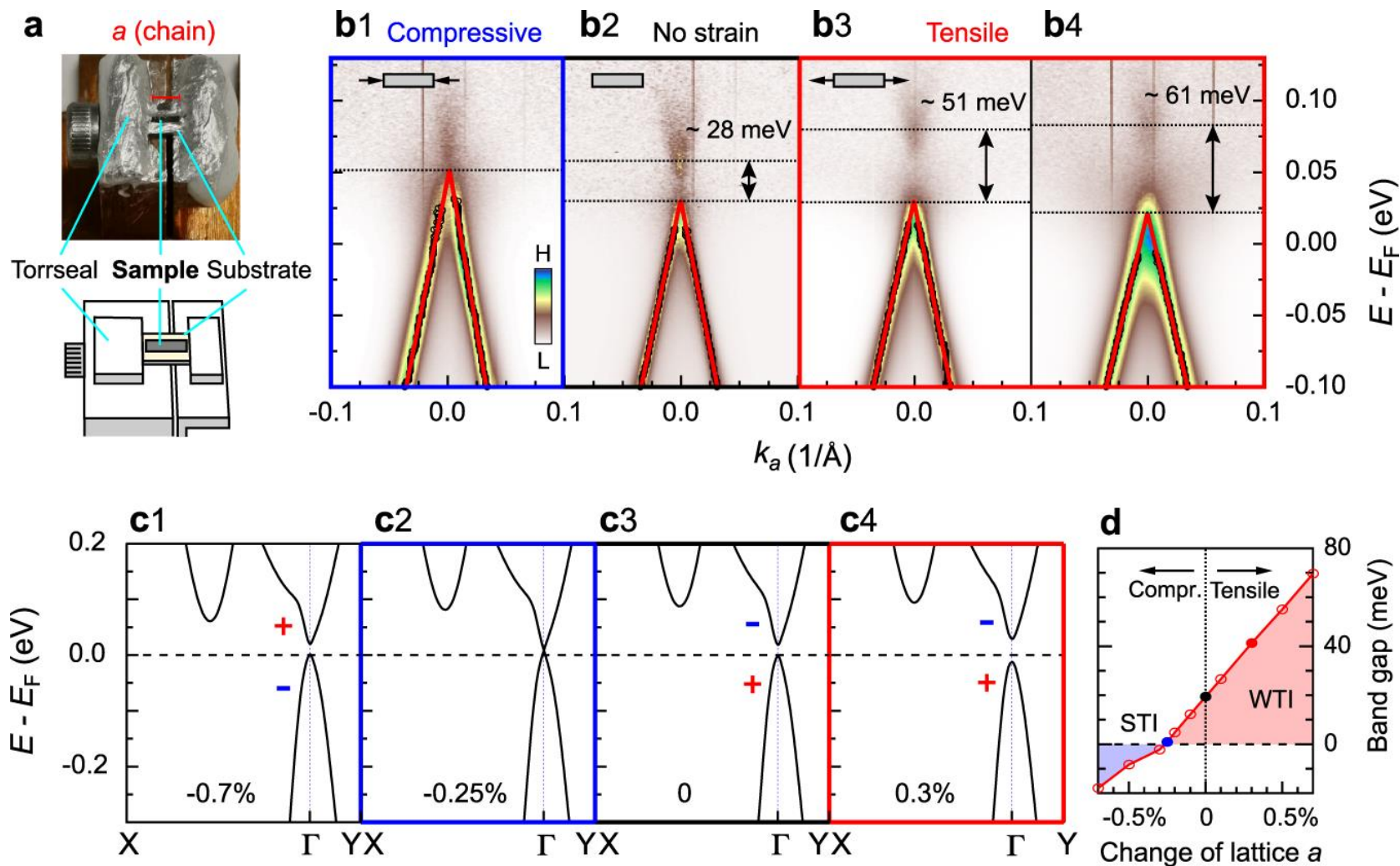
From transport measurements:



P. Lozano, QL et al., Phys. Rev. B 106, L081124 (2022)

For magnetic-field-induced Lifshitz transition in ZrTe<sub>5</sub> See S Galeski, QL et al Nature Communications 13, 7418 (2022)

# Strain Induced Topological Phase Transition in $\text{ZrTe}_5$



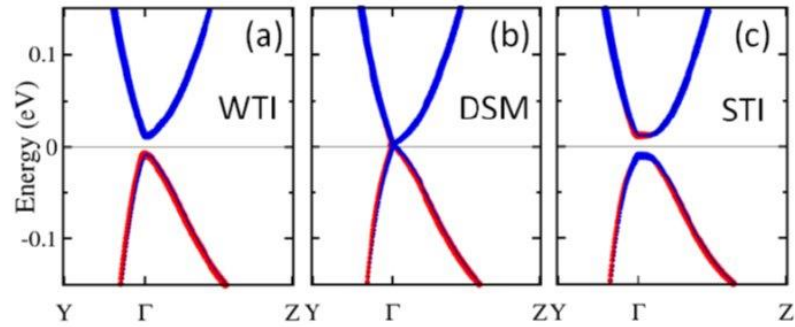
a) The strain device.

b) Bulk band gap change with compressive and tensile strain. The data are taken with p-polarized photons. The black markers are extracted from the MDC peaks, and the red solid lines are the fitting results

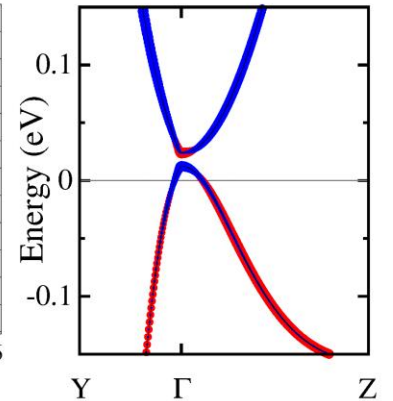
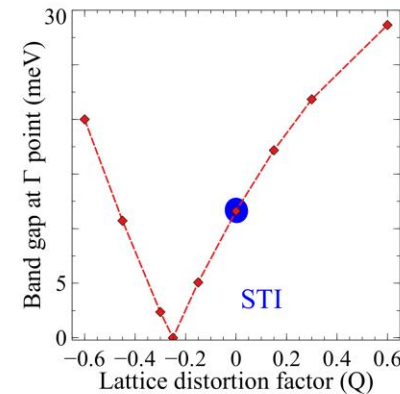
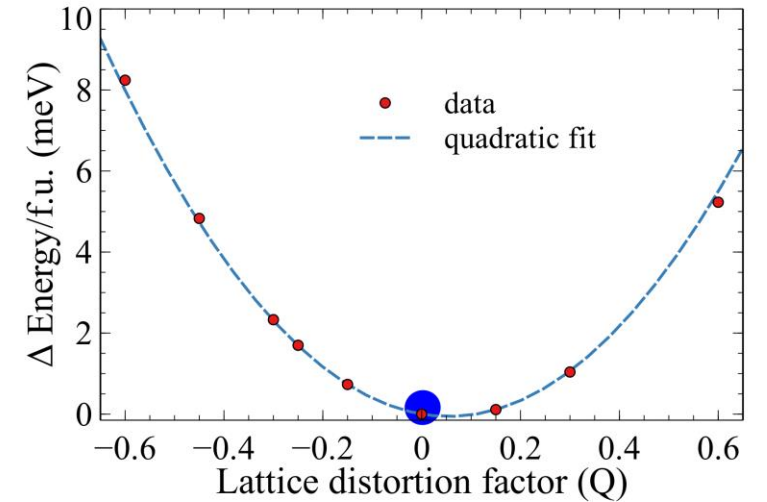
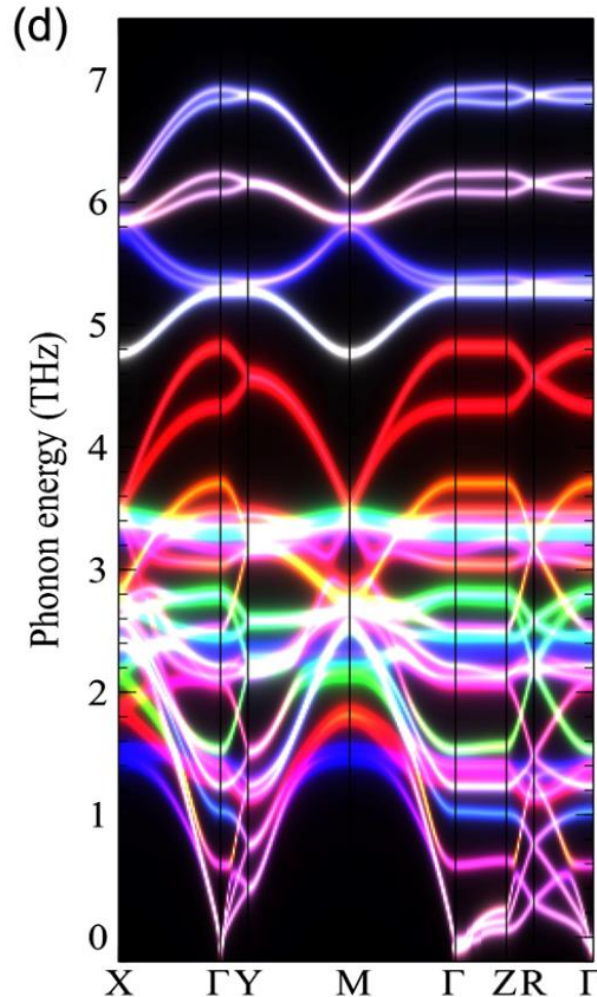
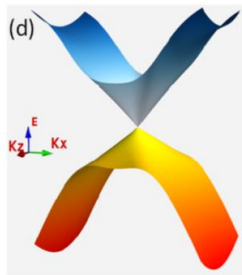
c) Calculated band structure with different lattice constant  $a$ . + and - signs indicate the parity of the two bands.

d) Calculated phase diagram with different lattice constant (strain). Blue, black, and red solid markers roughly indicate the experimental values in b.

# Coherent Phonon Control of Topological Phase Transition in $\text{ZrTe}_5$



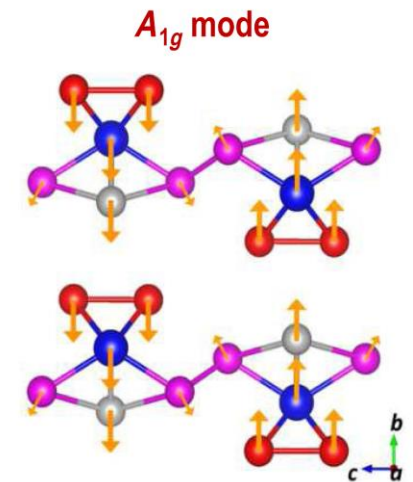
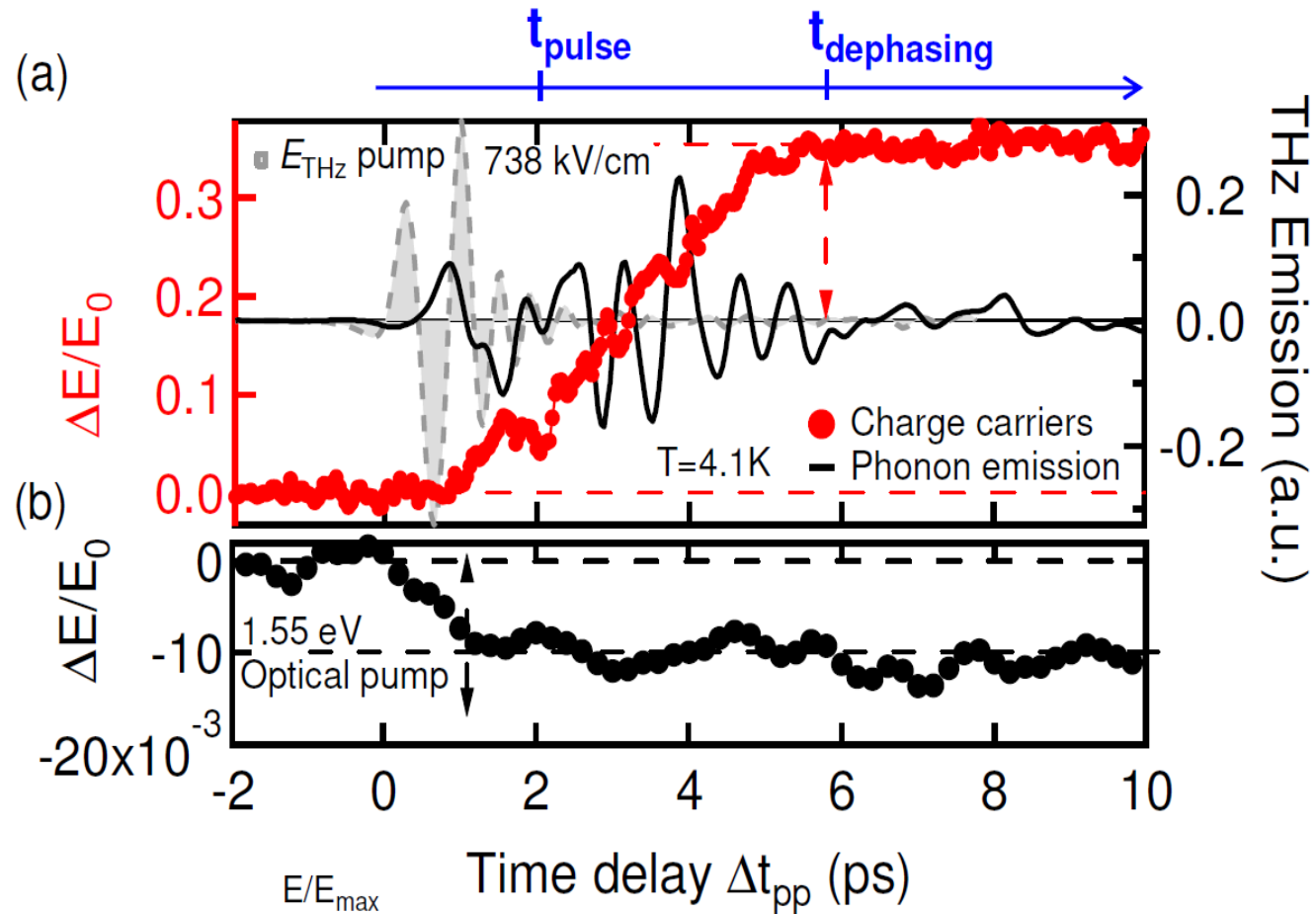
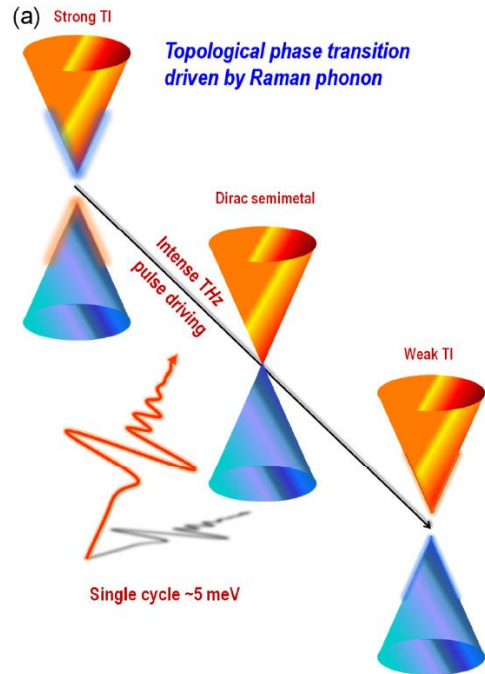
Evolution of the band structure around the  $\Gamma$  point for different values of the normal coordinate  $Q$  corresponding to the Ag-27 Raman-active phonon mode.



# Light-Driven Ultrafast Topology Switching in $\text{ZrTe}_5$

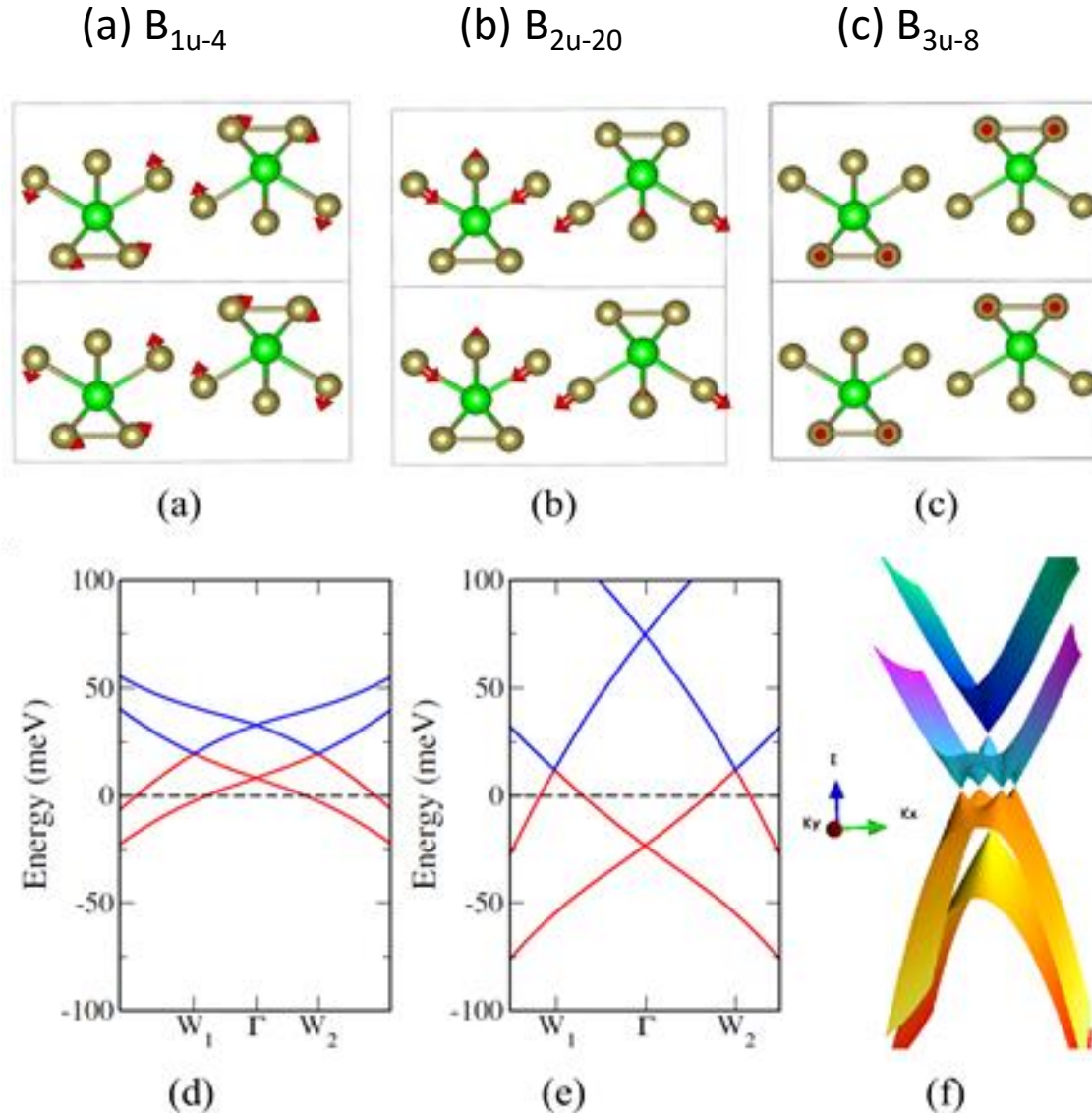


Prof. Jigang Wang  
(Ames Lab and  
Iowa State University)



Vaswani, QL, Wang, et al., Physical Review X 10, 021013 (2020)

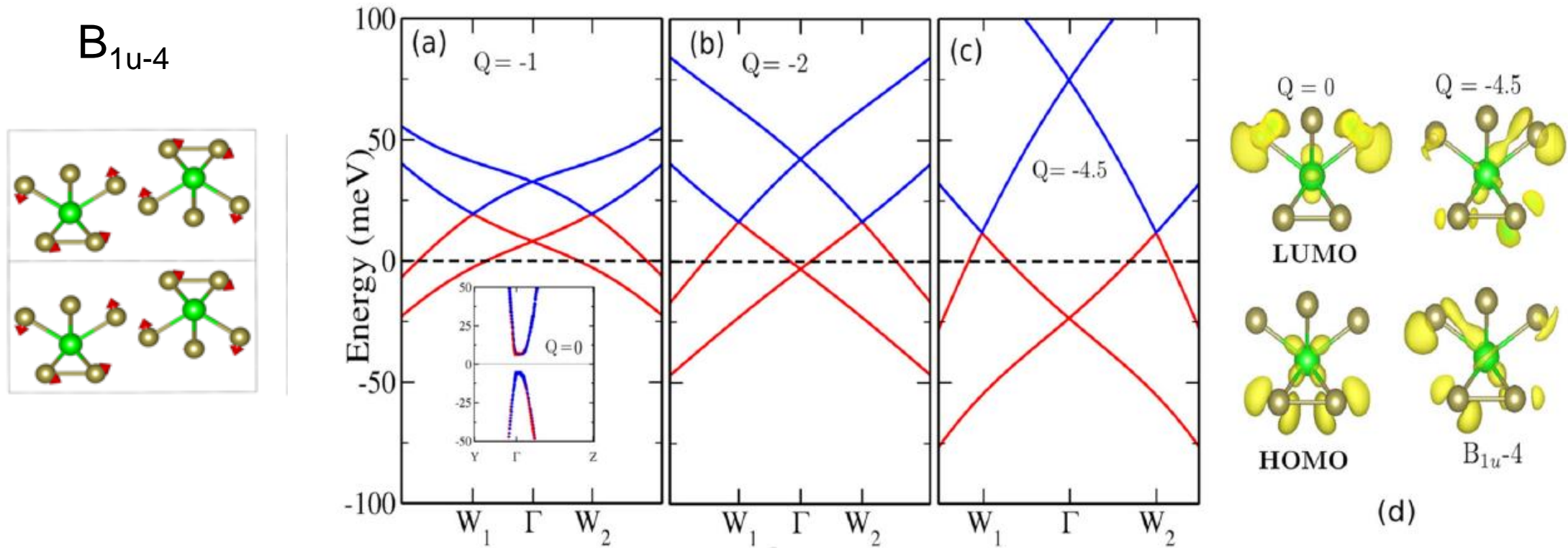
# Phonon induced Weyl phases in $\text{ZrTe}_5$



IR modes in  $\text{ZrTe}_5$  projected on the b-c plane: (a)  $B_{1u-4}$  (b)  $B_{2u-20}$  and (c)  $B_{3u-8}$ ; (d), (e) Band structure along  $W_1-\Gamma-W_2$  direction for  $Q$  values of 1 and 4.5 respectively calculated from DFT for  $B_{1u-4}$  mode. (f), the bands forming the WPs are shown on the  $k_x - k_y$ .

Aryal, Jin, QL, M. Liu, Tselik, and W. Yin, "Robust and tunable Weyl phases by coherent infrared phonons in  $\text{ZrTe}_5$ ," *npj Computational Materials* 8, 113 (2022).

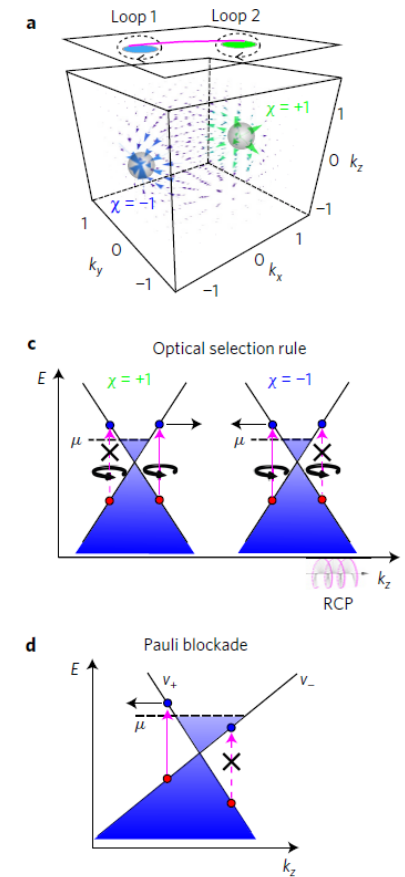
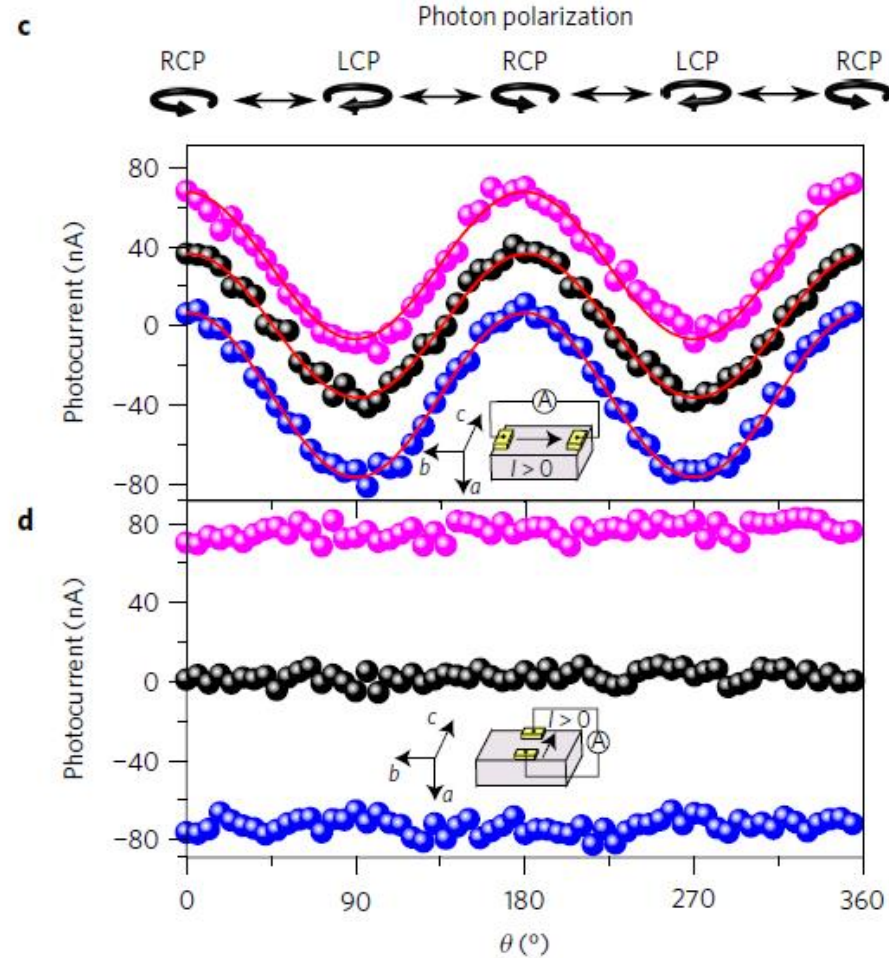
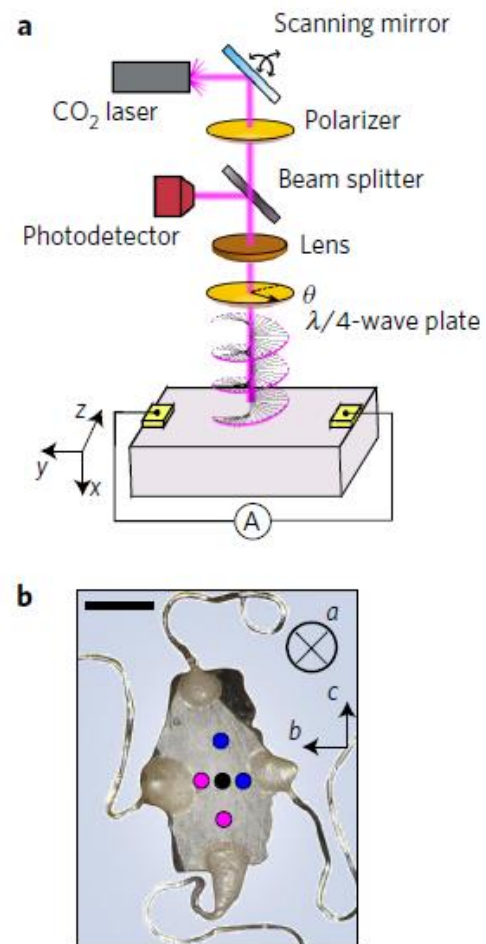
# Phonon induced Weyl phases in $\text{ZrTe}_5$



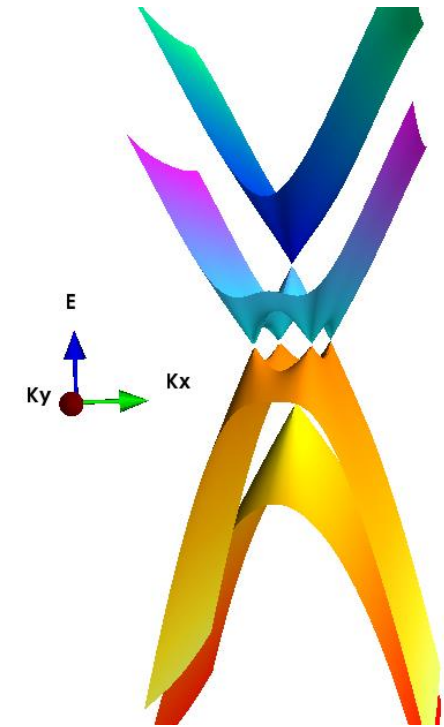
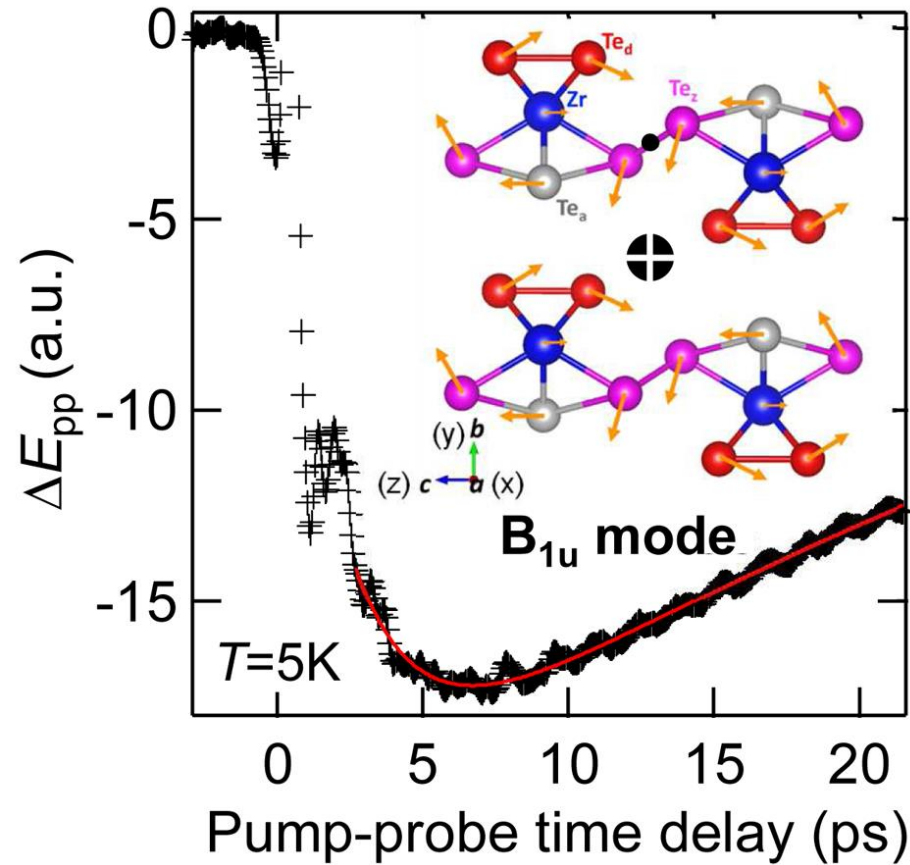
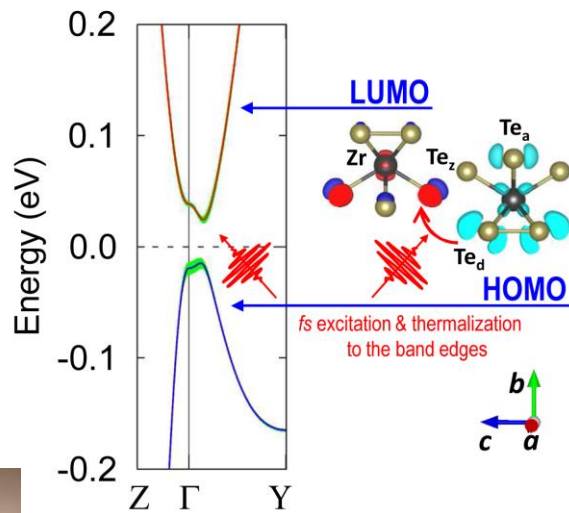
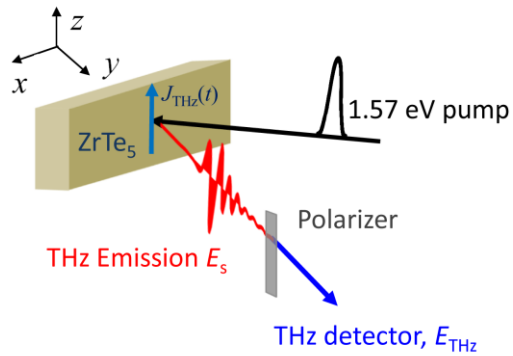
Aryal, Jin, QL, M. Liu, Tselik, and W. Yin, "Robust and tunable Weyl phases by coherent infrared phonons in  $\text{ZrTe}_5$ ," npj Computational Materials 8, 113 (2022).

# Detection and manipulation of chirality in Weyl semimetal TaAs

TaAs



# A Light-induced Giant Dissipationless Topological Photocurrent in $\text{ZrTe}_5$ \*



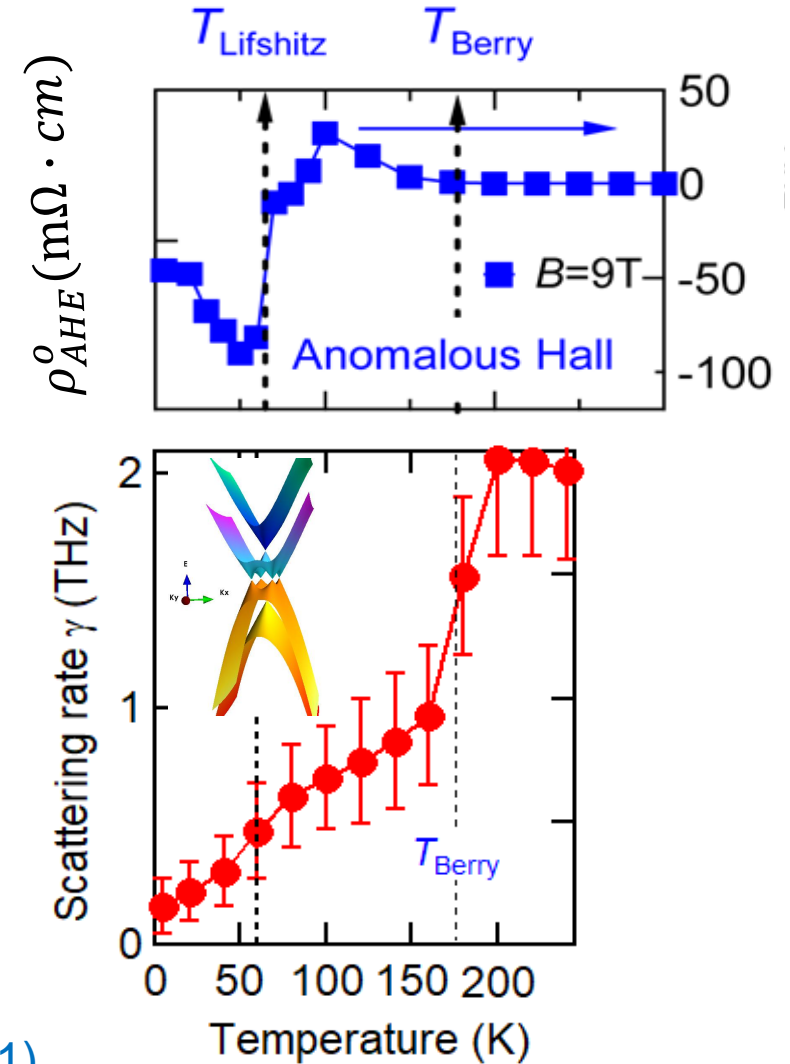
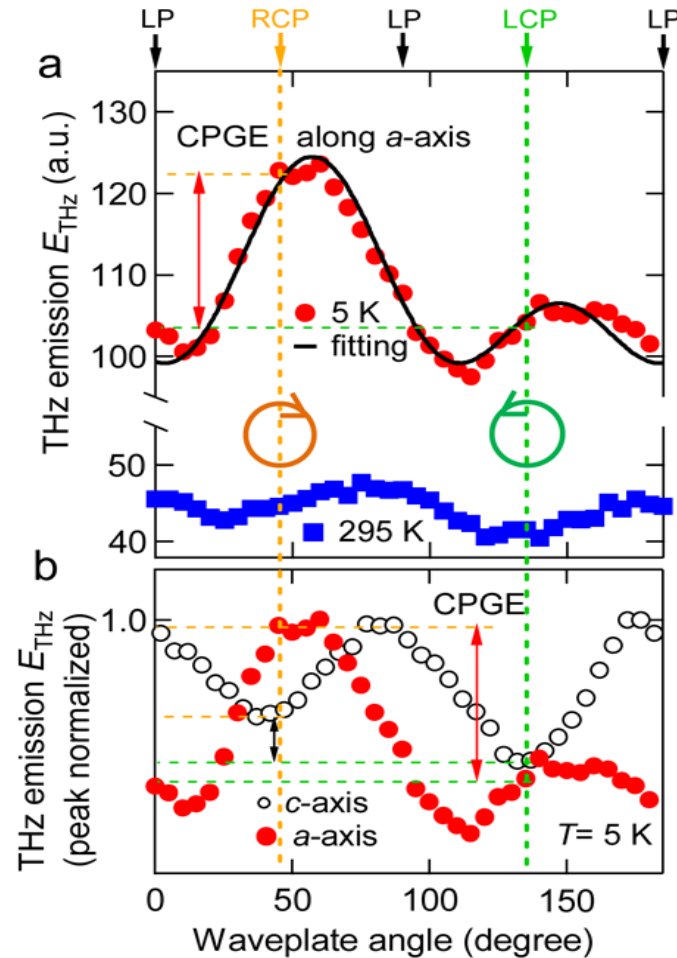
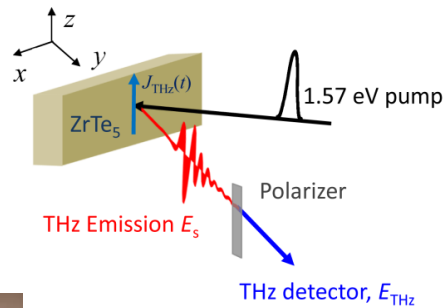
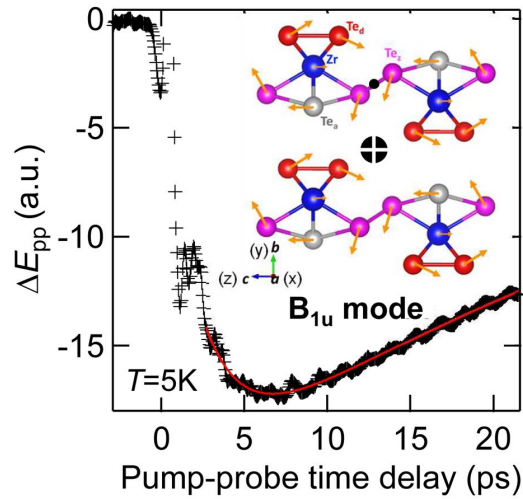
Aryal, QL, et al., npj Computational Materials 8, 113 (2022).

\*Luo, ..QL, Wang, et al., Nature Materials 20, 329 (2021)



Jigang Wang  
(Ames Lab/ISU)

# A Light-induced Giant Dissipationless Topological Photocurrent in $\text{ZrTe}_5$ \*



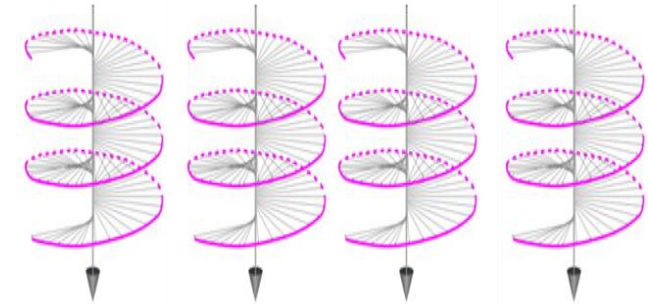
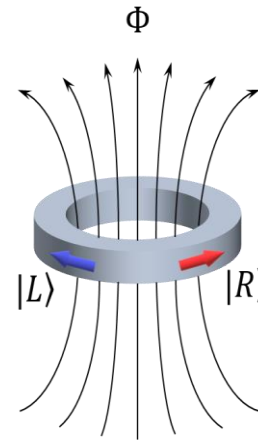
\*Luo, ..QL, Wang, et al., Nature Materials 20, 329 (2021)

# Chiral Qubit\*

Chiral Qubit is a micron-scale ring made of a Weyl or Dirac semimetal, with the two base states describing chiral fermions circulating along the ring clockwise and counter-clockwise. A fractional magnetic flux through the ring induces a quantum superposition. The entanglement of qubits can be implemented through the circularly polarized THz frequency electromagnetic fields.

$$\hat{H} = \hbar\omega \left( -i\partial_\theta + \frac{\Phi}{\Phi_0} \right) \hat{\sigma}_z.$$

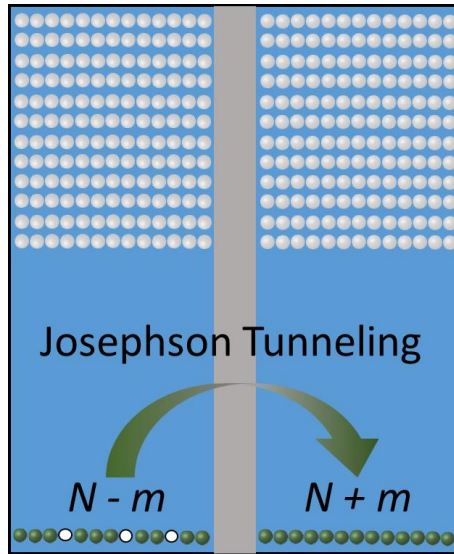
$$|0\rangle = \frac{1}{\sqrt{2}} (|R\rangle + |L\rangle), |1\rangle = \frac{1}{\sqrt{2}} (|R\rangle - |L\rangle)$$



$$\alpha |L\rangle + \beta |R\rangle$$

\*D. Kharzeev and QL “Quantum computing using chiral qubits” United States patent #10,657,456 B1 (2020);  
D. Kharzeev and QL “The Chiral Qubit: quantum computing with chiral anomaly” arXiv:1903.07133

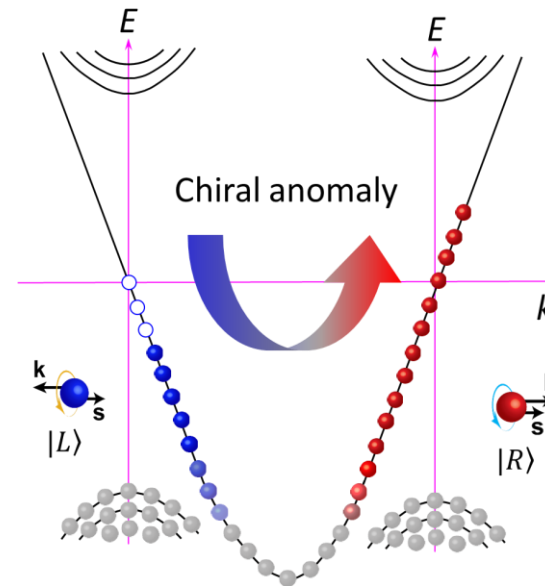
# Superconducting qubit



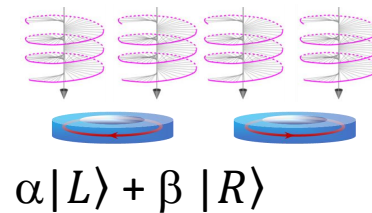
GHz energy gap  
Microwave pulse

1 K ~ energy fluctuations 20 GHz

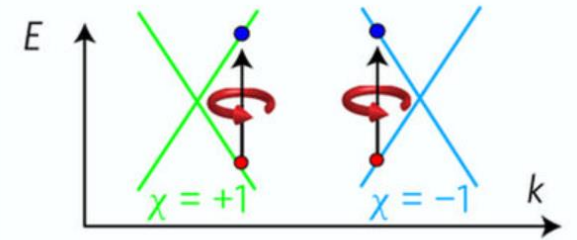
# Chiral qubit



THz pulse



Weyl—optical control



Weyl—electrical control

